# Glenohumeral joint and muscles functions during a lifting task

Najoua Assila[1,2,3], Sonia Duprey[1], Mickaël Begon[2,3]

[1]Univ Lyon, Université Claude Bernard Lyon 1, Univ Gustave Eiffel, IFSTTAR, LBMC UMR_T9406, F69622, Lyon, France
[2]School of Kinesiology and Exercise Science, Faculty of Medicine, University of Montreal, QC, Canada
[3]Sainte-Justine Hospital Research Centre, Montreal, QC, Canada

Submitted as an original article to the *Journal of Biomechanics*

Word count 3777

Address for correspondence:

Najoua Assila
School of Kinesiology and Exercise Science
Faculty of Medicine, University of Montreal
1700 rue Jacques-Tétreault,
Laval, QC H7N 0B6, Canada
Phone: +1 514 343 6111 (45172)
Email: najoua.assila@umontreal.ca

Key words: shoulder; rotator cuff; glenohumeral joint; muscle function; joint function

**ABSTRACT**

The mobility of the healthy shoulder depends on complex interactions between the muscles spanning its glenohumeral joint. These interactions ensure the stability of this joint. While previous studies emphasized the complexity of the glenohumeral stability, it is still not clear how the kinematics and muscles interact and adapt to ensure a healthy function of the glenohumeral joint. To understand the function of each muscle and degree of freedom of the glenohumeral joint in executing an above-the shoulder box handling task while ensuring stability, we adapted an index-based approach previously used to characterize the functions of the lower limb joints and muscles during locomotion. Forty participants lifted two loads (6 Vs. 12 kg) from hip to eye level. We computed the mechanical powers of the glenohumeral joint and its spanning muscles. We characterized the function of muscles and degrees of freedom using function indices. The function of the glenohumeral joint underlined its compliancy and design for a large range of motion, while the rotator cuff indices emphasized their stabilizing function. The overall muscle functions underlined the complexity of the glenohumeral stability that goes beyond the rotator cuff. Additionally, the load increase was compensated with changes in the functions that seem to favor joint stability. The implemented approach represents a synthetized tool that could quantify the glenohumeral joint and muscles behavior during tridimensional upper limb tasks, which might offer additional insight into motor control strategies and functional alterations related to pathologies or external parameters (e.g., load).

## INTRODUCTION

The upper limb is regularly recruited in daily activities. However, due to its neuro-musculoskeletal complexity, the understanding of its functional anatomy is still limited. With the evolution of the erect posture in humans, the upper limb evolved to ensure dexterous manipulation over a wide range of motion. Nevertheless, the upper limb is often recruited for load bearing activities, particularly during occupational handling tasks. The shoulder healthy function, particularly that of its glenohumeral joint depends on intricate interactions between its various muscles (Inman et al., 1996). In order, for shoulder muscles, to actuate and actively stabilize the glenohumeral joint throughout its large range of motion, they have long fascicle lengths, such that their working range remains within the force-length curve middle section (Veeger and van der Helm, 2007). While classical biomechanical approaches predict coordinates and moments of each joint degrees of freedom (DOF), as well as muscle activations and lengths, it is difficult to use their results to draw conclusions on the upper limb joint DOF and muscle behaviors during a handling task. Indeed, the variation of muscle force directions and moment arms during three-dimensional tasks hinders the identification of a sole muscle function. Additionally, while muscle behavior is strongly dependent on the force-length and force-velocity curves (Lappin et al., 2006; Richardson et al., 2005), using these curves to infer muscle functions during a dynamic task remains difficult due to their complex interactions. As muscle architectural features have an impact on its behavior, and thus on the joint function (Biewener, 2016), an approach that synthesizes muscle forces and length change is expected to shed a light on the upper limb function. According to Dickinson et al. (2000), muscle function can be split into four categories: strut, spring, motor and damper. A strut function expresses the capacity to generate large muscle forces (or joint moments) with little change in muscle length (or joint angle). Such behavior would be beneficial for rotator cuff muscles, particularly for their stabilizing action but not for joints

with large range of motion. A spring-like behavior expresses the capacity of a structure to store and release elastic energy; a motor-like behavior characterizes a structure that generates positive energy; while a damper-like behavior characterizes a structure that relies on muscle contraction to absorb energy. These four behaviors have been quantified through indices calculated using mechanical energy. While initially introduced for muscles, these categories have also been extrapolated to describe joint behavior. Indeed, this approach successfully identified lower limb joints and muscles functions during walking and running (Lai et al., 2019; Qiao and Jindrich, 2016). Implementing such approach to study the glenohumeral joint would shed a light on the upper limb motor strategies. However, as the healthy function of this joint relies on muscle co-contraction, predicting muscle forces that express the coactivation of muscles is critical to predict their function.

Our previous work on the effect of sex and load on the biomechanics of a lifting task presented the complexity of the upper limb biomechanics, as well as the interactions of the various biomechanical variables for a relatively straightforward lifting task (Bouffard et al., 2019; Martinez et al., 2020, 2019). While sex-load interactions were found for joint kinematics (differences linked to the load lifted by women), no sex-load interactions were observed for muscles' activations estimated using musculoskeletal models, nor for their electromyographic signals (EMG). Additionally, no load effect was observed for the relative time spent beyond a critical shear-compression dislocation ratio for the glenohumeral joint reaction force of all participants, despite the increased muscle activation. Local adaptations within the glenohumeral joint could explain the disparity of these results. Indeed, for pointing tasks, shoulder fatigue was reported to induce differences in the shoulder kinematics and in those of the trunk and elbow (Yang et al., 2019). Accordingly, an analysis of the adaptations within the glenohumeral DOF and muscle functions could explain why no changes are

observed for muscle activations and why seemingly the load does not impact the glenohumeral risk of dislocation.

The objective of this study is to further understand the glenohumeral joint and its muscles functions using an energy index-based approach during a lifting task. It was hypothesized from observation of the shoulder structure and function (multiple joints with scapulohumeral rhythm, large mobility range and muscles with long fascicles) that this approach should yield a minimal strut behavior for the glenohumeral joint DOFs irrespective of sex and load. On the other hand, scapulohumeral muscles, particularly the rotator cuff muscles that act as stabilizers, should mainly have a strut behavior. A secondary objective of this study is to analyze the effect of sex and load on the mechanical power and the predicted behaviors in light of our previous results regarding biomechanical parameters during a lifting task (Bouffard et al., 2019; Martinez et al., 2020, 2019). It is hypothesized that functional adaptations to load within the glenohumeral joint and musculature would occur. Particularly, an increase in the damper-like behavior of the joint DOFs and muscles is expected to counter the increased risk of injury associated with the increased load, pointing out complex adaptation strategies of the upper limb.

## METHODS

### *Data collection*

The raw data previously used by Martinez et al. (2020) was used. Forty participants who had no history of upper limb diseases performed a box handling task. The research protocol was approved by the University of Montréal ethics committee (n$^{o}$ 15-016-CERES-P). All participants provided their informed consent prior to the experimentation. A brief presentation of the experimental setup is described hereafter, see supplementary material for a detailed description.

The kinematics of the participants' trunk and right upper limb, and that of the box were tracked using 42 reflective markers. Bipolar surface EMG electrodes were used to measure the activation of 10 muscles: anterior, median and posterior deltoids, biceps, triceps, pectoralis major, latissimus dorsi, upper and lower trapezius and serratus anterior. Infraspinatus, supraspinatus and subscapularis activations were recorded using indwelling electrodes. The linear envelopes of the EMG signals were normalized to the maximal voluntary contraction (Dal Maso et al., 2016). The participants moved a box (6 or 12 kg) between two shelves from hip to eye level. Forces and moments between the right hand and the box were measured using a six-dimensional force sensor.

*Neuro-musculoskeletal model*

A musculoskeletal model was developed in Opensim (Delp et al., 2007) from the shoulder model of Wu (2016). The acromioclavicular and glenohumeral joints were both modelled as 3-DOF joints, while the sternoclavicular joint, the elbow and wrist were each modelled as 2-DOF joint. The glenohumeral joint DOFs sequence was plane of elevation, elevation and axial rotation (Wu et al., 2005). The generic model was first anthropometrically scaled to match the markers positions during a static trial in the anatomical position. The joint angles and moments were predicted using Opensim's inverse kinematics (a global optimization scheme with higher weights for markers that are reported to have a minimal soft tissue artefact) and inverse dynamics, respectively (Delp et al., 2007). Our study was focused on the glenohumeral joint DOFs and the muscles acting on it. Out of the 17 musculotendon units actuating the glenohumeral joint, three (teres major, teres minor and coracobrachialis) had no experimental EMG. The scaled models were further personalized by calibrating their neuromuscular parameters (e.g. optimal fiber length) using the CEINMS toolbox (Pizzolato et al., 2015). The personalized models were then used to predict muscle forces and fiber contraction velocities in CEINMS using an EMG-assisted scheme, while implementing a

fiber-tendon equilibrium constraint. The calibration and muscle force prediction processes are described in supplementary material.

*Analysis*

We calculated the glenohumeral joint 3-DOF powers as the product of their respective generalized moments and angular velocities. The muscle fiber power was calculated as the product of the fiber's tension and its contractile velocity. DOF and fiber powers were reported for men and women with both loads. To evaluate the function of each DOF and each fiber during the box-handling tasks, we calculated four indices that describe the mechanical behavior of an entity as a strut, a spring, a motor and a damper (i.e., function indices). The indices were defined to have a cumulative sum of 100% and are fully described in Lai (2019) and Qiao and Jindrich (2016). Further details about these indices can be found in supplementary material. Briefly, an entity that has a dominant strut behavior would generate large forces with little fluctuation in its length or angle. A spring-like behavior manifests itself with energy storage or release often synchronized with the compression and extension phases of the movement. Since the task of interest involved mainly a thoraco-humeral elevation, we defined the compression phase as the phase beginning with the lifting of the box from the shelf to the moment when the box is the closest to the participant, while the rest of the trial is the extension phase. An entity, acting like a motor, would generate mainly positive work throughout the task. Finally, a damper-like behavior would stand for a dominant negative work generation. To obtain dimensionless indices for muscle fibers, the strut index was normalized with respect to the fiber's optimal length obtained with the model calibration.

The effects of sex and load on the glenohumeral DOF and muscle fibers powers, as well as their function indices were evaluated using a two-way nonparametric ANOVA with repeated measures on the load (Pataky et al., 2015). Statistical significance was fixed at 0.05. For the 1D analysis, the family-wise error for all clusters was respected using a Bonferroni correction

to account for the number of DOFs and muscle. On the other hand, the p-values reported for the function indices (0D analysis) are the ones obtained from a Holm-Bonferroni correction, to maintain the power of the analysis, despite running the tests for four indices.

## RESULTS

The sex had no significant effect on the joint power, while the load had a significant effect on the power of the glenohumeral elevation ($p < 0.05$; Fig. 1). The glenohumeral plane of elevation and axial rotation had power peaks higher than those calculated for the elevation. These peaks occurred close to the transition from the compression to the extension phase (Fig. 1). The net joint power was mainly the result of the anterior deltoid, biceps and latissimus dorsi fiber powers, followed by the infraspinatus and supraspinatus, two rotator cuff muscles (Fig. 2). No major effects of sex, load, nor their interaction were observed on the fibers power.

All glenohumeral DOF had a minimal strut-like behavior with no significant effect of sex or load ($p > 0.05$; Fig. 3). The spring-like behavior was not a main function for any of the DOF; however, it was usually more present in the glenohumeral axial rotation, irrespective of the load or sex ($p > 0.05$). The load affected the elevation damper ($p = 0.012$) and motor ($p = 0.035$) behaviors. Both men and women relied on their glenohumeral plane of elevation and elevation as prime motors. For the 6 kg lifting task, women relied more on their plane of elevation to drive the motion with a motor index of 66 ± 15%, whereas men preferred their glenohumeral elevation (68 ± 23%). For the 12 kg task, women did not change their power strategy (glenohumeral plane motor index: 60 ± 16%), while men moved the box by using both their plane of elevation (48 ± 20%) and elevation (46 ± 28%) as motors. The damping action was ensured by the glenohumeral axial rotation for women and men during the 6 kg trial. However, as the load increased, so did the damping action of the two other DOFs.

Most muscles had a mainly strut-like behavior, with rotator cuff muscles showcasing the highest values (on average 90%). The biceps had, almost, no strut-like but a spring-like behavior irrespective of the trial, followed by the posterior deltoid (Fig. 4). Following the strut-like behavior, the muscles had either a damper or a motor-like tendencies, except for the bicep's fibers. The clavicular head of the pectoralis major had a motor-like behavior for all trials. The load also had an effect on the damping behavior of the latissimus dorsi and subscapularis ($p<0.015$), on the spring behavior of the posterior deltoid and the infraspinatus ($p<0.015$) and the strut behavior of the posterior deltoid, subscapularis and biceps ($p<0.015$). An effect of the interaction sex-load was only observed on the biceps strut behavior ($p<0.015$).

## DISCUSSION

We implemented an analysis of the glenohumeral joint DOF and its muscle fibers based on their mechanical energy to improve our understanding of the glenohumeral joint functions during a lifting task. The predicted behavioral indices provided evidence supporting our hypotheses regarding glenohumeral DOF and muscle functions. The limited strut indices of the glenohumeral joint highlighted its large range of motion, whereas the large strut behavior of muscle fibers, particularly the rotator cuff, emphasized their stabilizing function. Finally, the predicted indices highlighted the sensitivity of kinematic and activation strategies to load and sex.

### *Glenohumeral joint: a design for a wide range of motion*

The complexity of the glenohumeral joint morphology has evolved to ensure a large range of motion (Larson, 2009). With thoracohumeral elevation, the scapula is reoriented to maintain congruency with the humeral head, and the humerus is externally rotated to avoid impingement (Ludewig et al., 2009; Stokdijk et al., 2003). The effect of the scapula

orientation can be observed in the power evolution of the glenohumeral DOFs. While the task involved mainly a change in potential energy of the box (thoracohumeral elevation) (supplementary data, Fig. S3), the power of the glenohumeral elevation was smaller than the other DOFs. Additionally, the occurrence of power peaks close to the transition between pulling and pushing the box pointed out a strategy where participants relied on a sudden increase in the box momentum to drive its elevation, confirmed by the change in box vertical velocity. Women, who exhibit less upper body strength than men (Janssen et al., 2000), had a steeper increase of the box vertical velocity at this transition (supplementary data, Fig. S4). This could potentially explain the increased risk of injury for women, as the upper-arm velocity was correlated with shoulder complaints (Balogh et al., 2019).

The design of the glenohumeral joint to cater to both mobility and stability can be observed in its DOF strut coefficients. The box handling task did not reach extreme upper limb positions yet was highly demanding of the shoulder. However, the strut index remained relatively low, suggesting that the glenohumeral joint has a high compliancy, which would facilitate the upper limb motor control and movement regulation. This is coherent with the glenohumeral joint architecture that is optimal for large and precise displacements (Arias-Martorell, 2019). This optimization impacted strongly the orientation of the scapula, which has been linked to the throwing function of the upper limb, and enabled the use of elastic energy stored during external rotation to increase the power generated for high-speed throwing (Roach et al., 2013). This could possibly explain the high spring index observed for the humeral axial rotation. Besides its spring function, the axial rotation behaved mainly as a damper, which could point out functions of the passive structures (shoulder capsule and ligaments) that would behave mostly as elastic components, stiffening with the glenohumeral axial rotation (Burkart and Debski, 2002; Wilk et al., 1997). As the load increased, this passive damping was probably no longer enough, thus the increase in the other DOFs input to the damping, and

possibly glenohumeral stability, at the expense of the elevation's motor behavior, and the box vertical velocity.

*Adaptations to load within the joint*

The main motor behavior was ensured by the glenohumeral elevation and plane of elevation. Women opted to use their glenohumeral plane of elevation to drive the movement. While their strategy did not change between loads, men adapted theirs as the load increased, distributing the motor load more equally between the actuators of the glenohumeral elevation and plane of elevation. Participants have been reported to increase the use of their lower limbs with load increase, with men relying on their hip vertical displacement more than women (Martinez et al., 2020). The 12 kg task might have been taxing for both men and women's glenohumeral joint. For men, however, relying on their lower limb, they decreased the motor demand on the glenohumeral elevation, favoring stability. Women, on the other hand, might have already strained their shoulder for the 6 kg task, which led them to seek assistance from their elbow for the 12 kg one (Martinez et al., 2019). This observed adaptation could possibly shed a light on neural control schemes that could start within the same structure (glenohumeral), before seeking neighboring ones (distal joints). This points out the importance of the coupling of a local and global kinematic analysis to gain a deeper understanding of the human motion.

*Fiber power adaptation to load*

Unlike joint power, the fiber powers did not have any significant increase with the load, despite the significant muscle activation increase shown in Bouffard et al. (2019). This power invariance pointed out a possible decrease in the fiber contraction velocity as the load increased. This could be a direct effect of the decrease of the glenohumeral range of motion with the load (Martinez et al., 2019). This decrease could also be linked to the change in compliance of the muscle-tendon unit. As the load increased from 6 to 12 kg, the stiffness of the tendon might have increased (Raiteri et al., 2018), impacting the fiber compliance, which

is reported to affect its power generation and efficiency (Fenwick et al., 2017). This potential adaptation strategy would decrease injury risk at higher loads. As women have more compliant tendons compared to men (Kubo et al., 2003), this could account in part for women's higher injury rate, particularly as they rely more on speed to drive the box.

*Fiber function between actuation and stability*

The highest strut like behavior in muscles was showcased by the infraspinatus and subscapularis. This was consistent with their architecture, having relatively short fibers and large physiological cross-sectional areas, which enables them to generate large forces over a short range of deformation (Gobbi, 2017). Overall, most of the muscles displayed a strut-like behavior for the studied task, which implies a high fiber force with a minimal length change, which supports our initial hypothesis. Unlike most upper limb muscles, the biceps had a main spring-like behavior, storing and releasing energy. This behavior is consistent with its architecture, as slender muscles with long tendons are reported to be favorably designed for energy saving (Biewener, 2009). However, mechanical energy storage remains costly from a chemical energy perspective.

The muscle ability to quickly actuate a joint depends on the speed and the type of contraction. As reported by Tillin et al. (2018) and Aagard et al. (2018), the change in fiber velocity per degree of joint rotation is different depending on the type of contraction. They showed that muscles would more efficiently generate a higher torque during concentric activations at higher speeds (Tillin et al., 2018). This might explain the significant decrease in the motor function of the clavicular head of the pectoralis major as the load increased, since the contraction velocity decreased, limiting the fiber force potential. This could also explain why women chose to approach the box to their trunk, as it gave them higher potential for a concentric explosive contraction. However, an explosive contraction without sufficient muscle strength and control, particularly for higher loads, might increase injury risk (Davies

and Matheson, 2001). This might explain why the damper behavior of some muscles increased with the load, as this function should help in the stabilization of the humeral head. The effect of the load on the strut, spring and damper behavior further points to the complexity of the glenohumeral joint stabilization, as it involves more than just the rotator cuff muscles (Lee and An, 2002; Yanagawa et al., 2008).

*Energetic approaches to complement the upper limb understanding*

The musculoskeletal structure is a transducer that converts chemical energy into mechanical work (Wilkie, 1975). Accordingly, energetic approaches could potentially offer a complementary and insightful understanding to the classical biomechanical analysis of forces and kinematics (Guo et al., 2003; Siegel et al., 2004). Similarly, within our study, we could gain insight into the intricate functions of the different glenohumeral joint DOF, without the need to analyze unidirectional movements (Hawkes et al., 2019). The use of the four function indices enabled a fair analysis of the different muscles within their physiological abilities. Indeed, while the infraspinatus and subscapularis had low power magnitude, their role in glenohumeral stability was emphasized by their strut index. This reinforces our understanding of the stabilizing potential of the rotator cuff muscles, particularly as their characteristics are still not well understood (Sangwan et al., 2015). These indices could also be used in the development of ergonomic work strategies that go beyond the joint repartition (Martinez et al., 2020) of the task.

Our study had some limitations. We chose to normalize the shelves height to the participants to reduce bias against women. For an energetic approach, this led to differences in the potential energy of the box. However, it was expected that the gender-related differences would only be exacerbated in a working environment. The use of an energetic approach is also limited by the power magnitude sensitivity to the scapula kinematic errors, particularly those related to the soft tissue artefact (Blache et al., 2016). As for the indices' definition, the

main limitation relied in the need of a compression and extension phases within the studied trial. While this could be relatively easy to define for cyclic tasks: such as handcycling, it is less straightforward for the majority of the upper limb tasks. Finally, the strut index is defined relatively to a given length that could change the overall distribution of the muscle functions. Unlike in Lai et al. (2019), there is no specific known behavior of the upper limb tendons or muscles. Accordingly, we decided to use the fiber optimal length to make the strut index dimensionless. This choice should circumvent introducing any task, participant or muscle induced bias to the study. In the future, more research needs to be done to find an optimal parameter for normalizing the upper limb strut index.

The implemented index-based approach enabled a more comprehensive understanding of the upper limb motor control strategies during a box handling task and a summarized insight in the function of the various muscles. The indices highlighted particularities of the glenohumeral joint (large range of motion) and its muscles (stabilizing function), as well as sex-dependent adaptation strategies to load, supporting our initial hypotheses. This approach might improve our understanding of the upper limb by offering additional insight into its motor control strategies, its components functional alterations related to pathologies or its adaptations to external parameters.

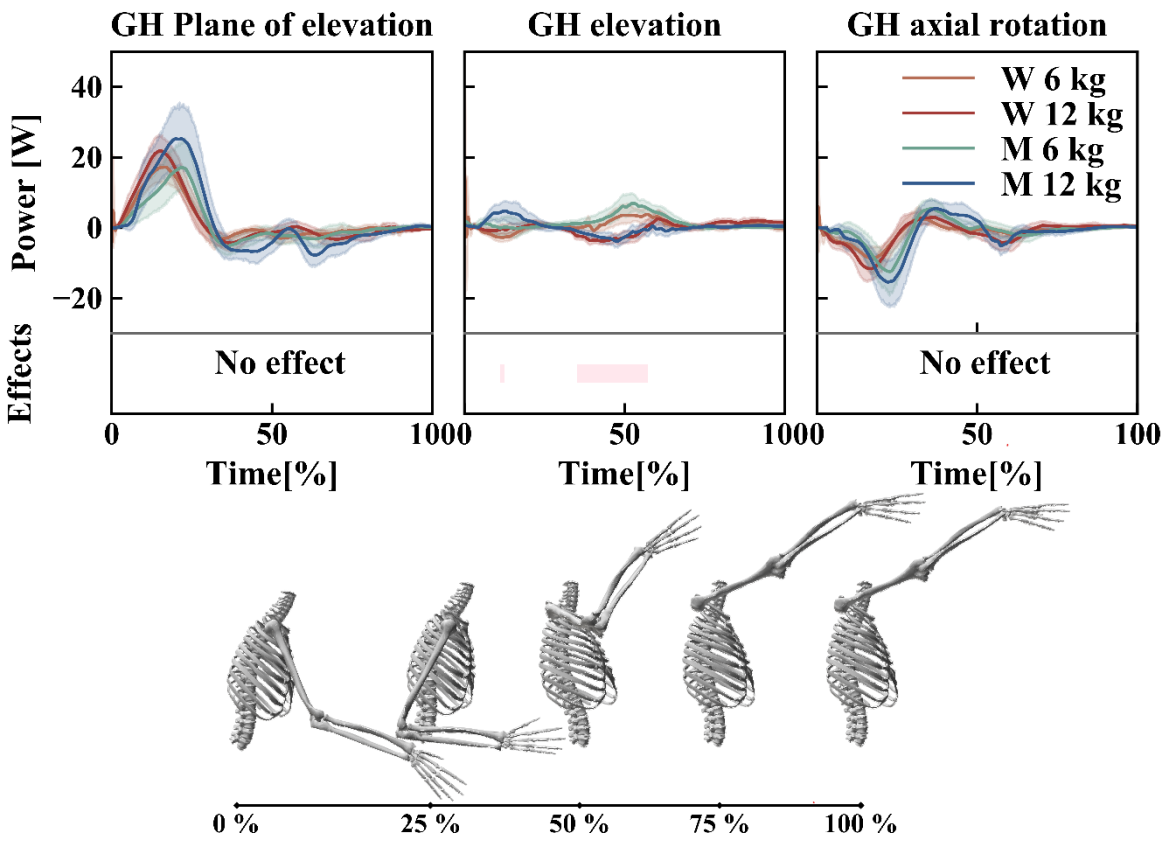


*Fig. 1. Glenohumeral joint power generated by women (W) and men (M) during the box (6 or 12 kg) lifting tasks: solid line: mean value, hue: 95% confidence interval. In the bottom part of the graphs, pink bands correspond to the load effect.*

294 –

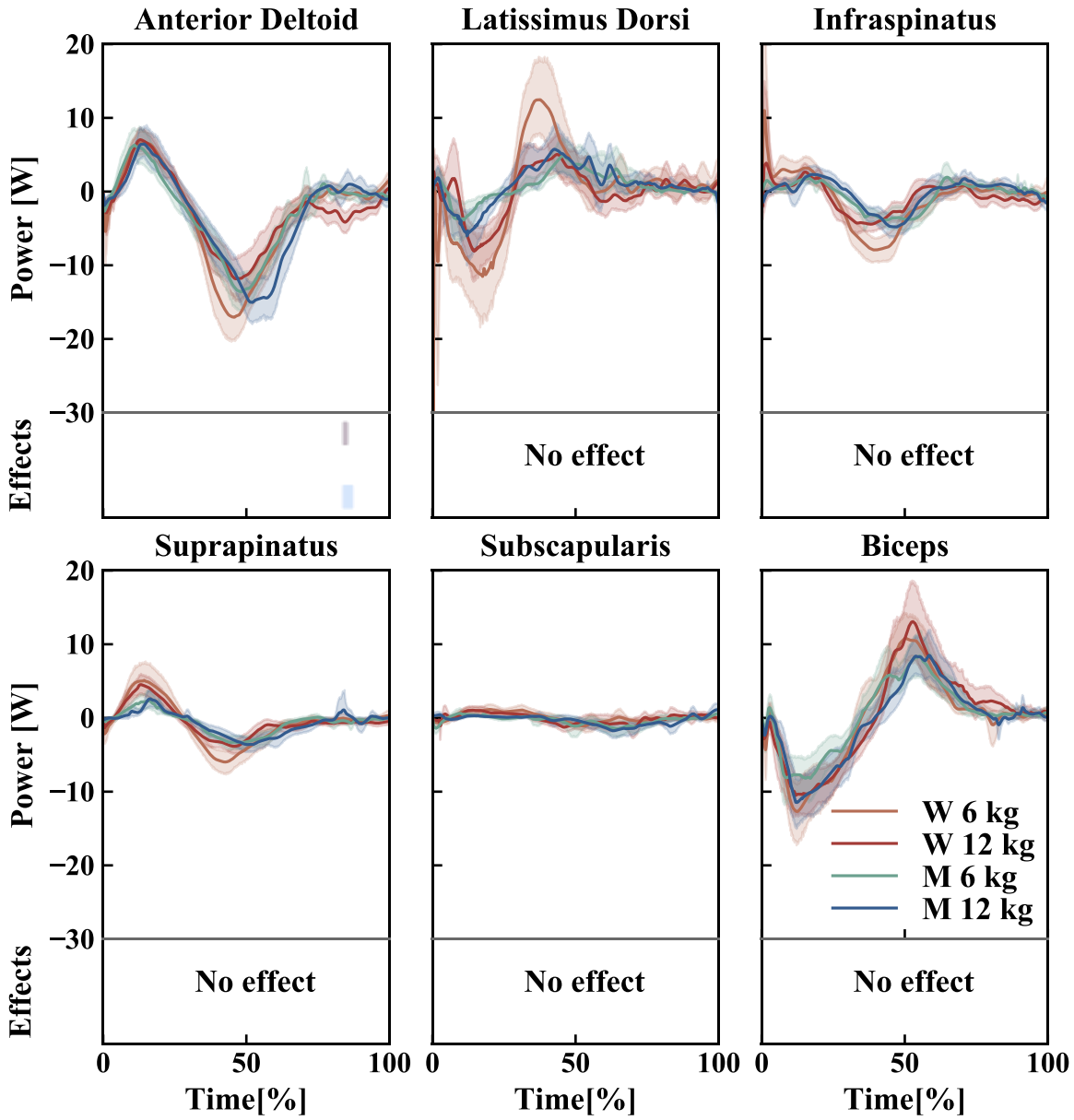


295

296 *Fig. 2. Power generated by muscle fibres during the box (6 and 12 kg) lifting tasks for women*

297 *(W) and men (M); solid line: mean value, hue: 95% confidence interval, blue bands: sex effect,*

298 *purple bands: sex-load effect.*

299

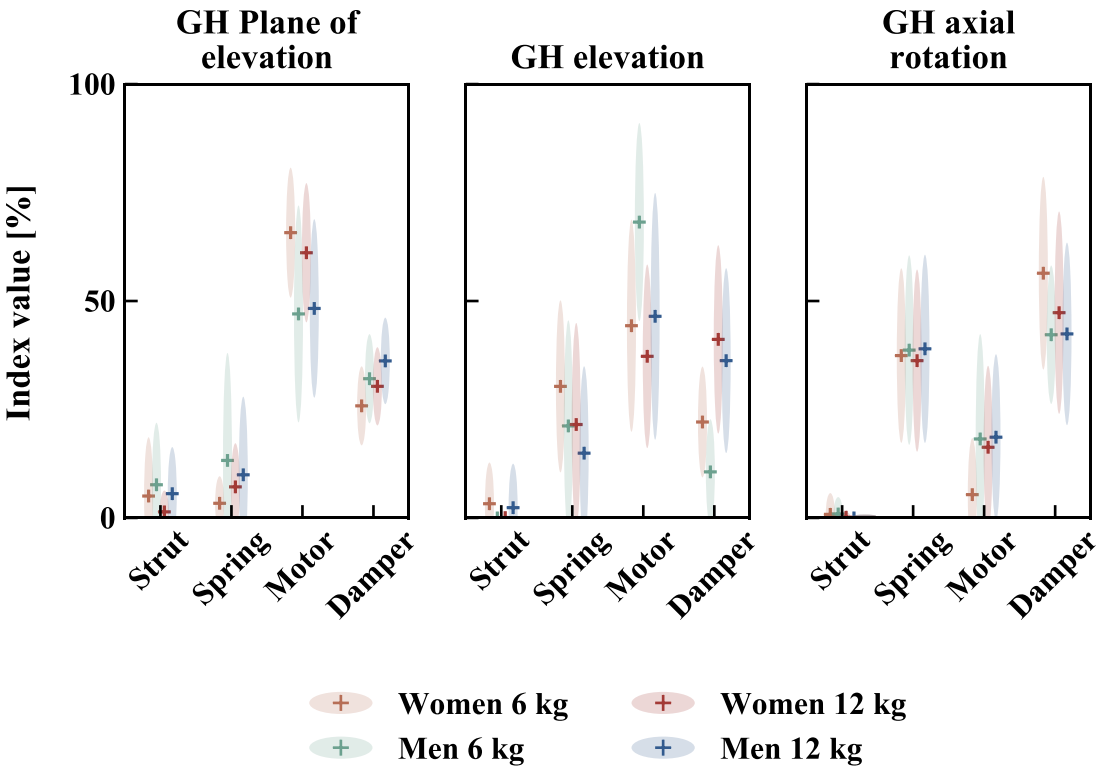


300

301 *Fig. 3. Mean values of the four joint indices with a load of 6 and 12 kg for women and men.*

302

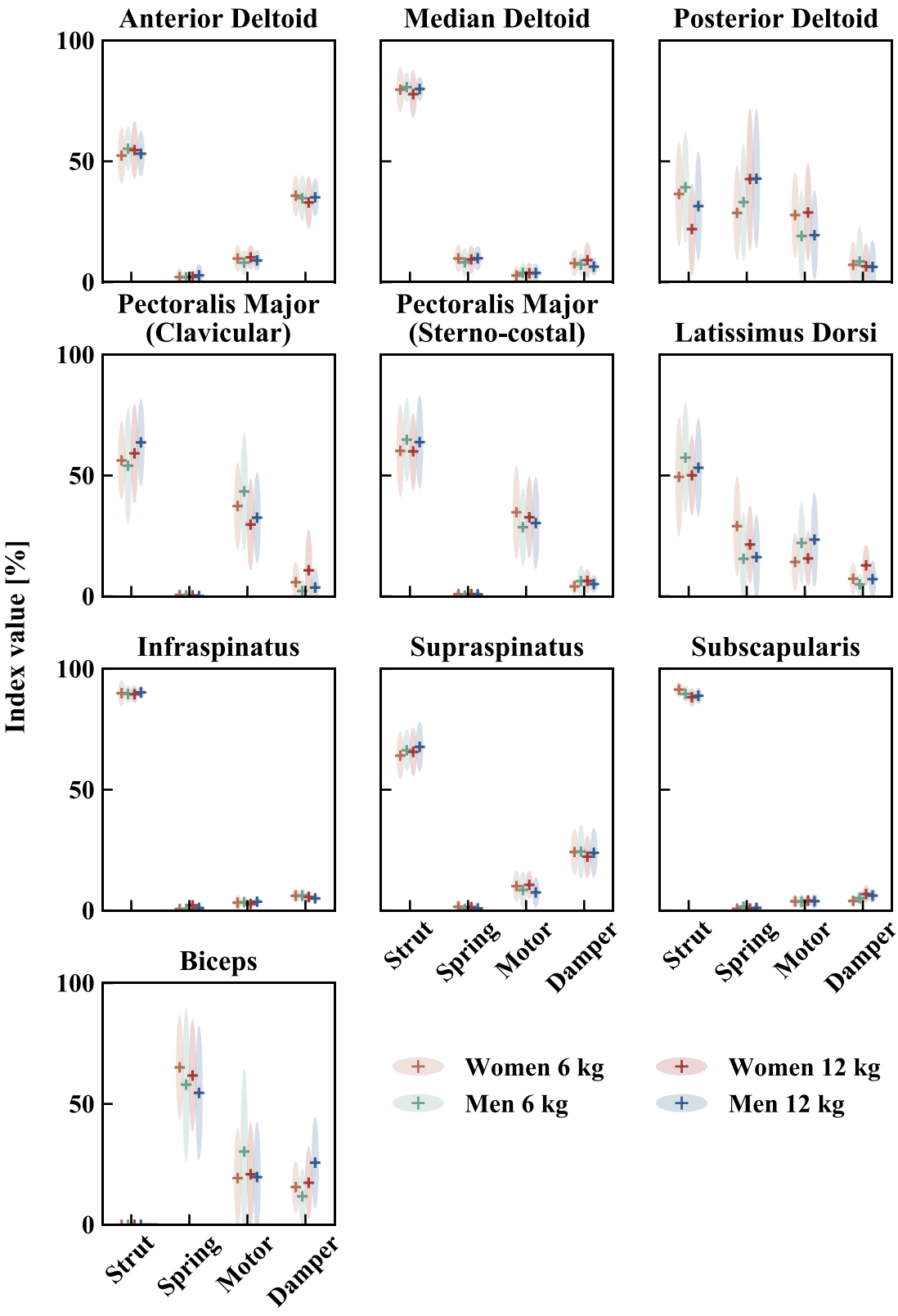


303

304 *Fig. 4. Mean values of the four muscle fiber indices with a load of 6 or 12 kg for women and*

305 *men.*

**SUPPLEMENTARY MATERIAL**

*Data collection*

Forty participants (20 women; 23.12 ± 3.1 years; 173.5 ± 9.5cm; 68.1 ± 12.7) took part in this study. They did not suffer from any significant disability related to their upper limbs or backs. The participants first performed a static trial to anthropometrically scale the musculoskeletal model. Then, they moved a box from a shelf at hip level to a shelf at eye level. The shelves heights were adjusted to the height of each participant. The participants performed three lifts for each mass (6 and 12 kg). The order of the lifts was randomized. A 30 s rest period between lifts was given for recovery with increased time if needed. Assuming symmetry between the right and left side during this task, only the right side was analyzed. A 6-degree-of-freedom force sensor (Sensix, Poitiers, France) was mounted on the right handle of the box to measure the contact forces between the box and the participant's hand. A threshold of 5 N was used to detect the start and end of each trial. Following the recommendations of Jackson et al. (2012), 34 reflective markers were used to track the trunk and upper limb kinematics (Fig. S1). Eight markers positions on the box corners were used to track the box kinematics.

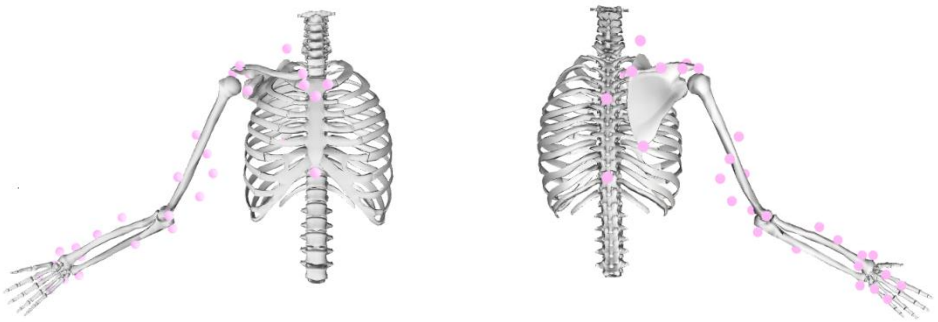

*Fig. S1. The position of the markers used to track the trunk and upper limb kinematics.*

*Neuro-musculoskeletal model*

To personalize the neuro-musculoskeletal model, the various parameters involved in the activation and contraction dynamics were calibrated using experimental EMG, namely:

- The two recursive coefficients of the second-order differential system that relates the excitation to the neural activation

- The shape factor that related the neural activation to the muscle activation

- The fiber optimal length

- The tendon slack length

- The isometric maximal force.

One trial per participant lifting a 6 kg load was used for calibration. The calibration aimed to find musculo-tendon parameters that simultaneously minimized the inverse dynamic torques tracking quadratic error and the ratio of the glenohumeral joint shear to compressive contact forces, while driving the model using the experimental EMG. A penalty was used to avoid normalized fiber length outside the physiological range throughout the calibration trial. This objective function enabled the respect of the glenohumeral joint non-dislocation constraint without the need to explicitly include it in the muscle force prediction algorithm (Assila et al., 2020).

The calibrated models were then used to predict muscle forces through an EMG-informed algorithm (Fig. S2). The optimization scheme adjusted the available experimental EMG envelopes and synthesized the excitations that were not measured experimentally. The adjusted and synthesized excitations minimized three terms: 1- inverse dynamics joint moments tracking error, 2- experimental envelopes tracking error, 3- the sum of squared excitations for all lines of actions. The weights used for the various terms were chosen to achieve a good balance between joint moments and excitations tracking (Sartori et al., 2014). At the contraction dynamics stage, the muscle-tendon equilibrium is accounted for by solving the equality of the tendon and fiber forces with the fiber length as parameter. The root of this equation is found using Brent's method (Brent, 1973).

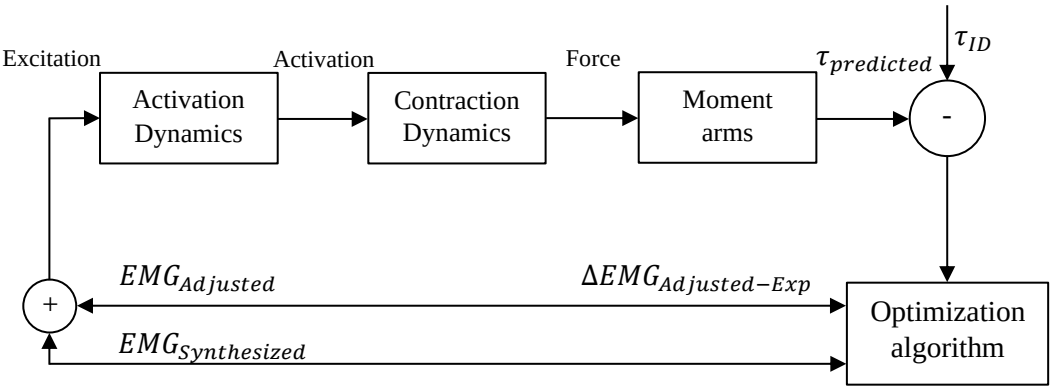


*Fig. S2. Overview of the muscle force prediction algorithm. $\tau_{ID}$ is the moment obtained from inverse dynamics that the algorithm tries to track, $EMG_{Adjusted}$ is the adjusted excitation of the muscles that had experimental data, whereas $EMG_{Synthesized}$ is the excitation of the muscles that had no experimental data.*

*Function indices*

The function indices calculation was based on the formulae presented in (Lai et al., 2019; Qiao and Jindrich, 2016). The strut index is the ratio of the mechanical work generated by the entity during the box lifting task to the sum of the force norm generated. Accordingly, the index can be defined as follows:

$$I_{strut,DOF} = \max\left(1 - \frac{\left(t_{end} - t_{beg}\right)\int_{t_{start}}^{t_{end}} |P_{DOF}|\, dt}{\int_{t_{start}}^{t_{end}} |M_{DOF}|\, dt}, 0\right) \times 100\%$$

$$I_{strut,muscle} = \max\left(1 - \frac{\left(t_{end} - t_{beg}\right)\int_{t_{start}}^{t_{end}} |P_{muscle}|\, dt}{l_{opt}\int_{t_{start}}^{t_{end}} |F_{muscle}|\, dt}, 0\right) \times 100\%$$

with $P_{DOF}$ and $P_{muscle}$ the mechanical powers of the DOF and the fiber, respectively; $M_{DOF}$ the DOF moment and $F_{muscle}$ the fiber force. The optimal length of the fiber ($l_{opt}$) was used to obtain a dimensionless index. The lifting task started at $t_{beg}$ and finished at $t_{end}$.

The other indices were calculated similarly for both the glenohumeral DOFs and muscles. They were calculated as follows:

$$I_{spring} = \frac{2.\min(|W_{com}^{-}|, |W_{ext}^{+}|)}{|W_{tot}^{+}| + |W_{tot}^{-}|} \times (100\% - I_{strut})$$

$$I_{motor} = \frac{|W_{tot}^{+}| - \min(|W_{com}^{-}|, |W_{ext}^{+}|)}{|W_{tot}^{+}| + |W_{tot}^{-}|} \times (100\% - I_{strut})$$

$$I_{damper} = \frac{|W_{tot}^{-}| - \min(|W_{com}^{-}|, |W_{ext}^{+}|)}{|W_{tot}^{+}| + |W_{tot}^{-}|} \times (100\% - I_{strut})$$

where $|W_{tot}^{+}|, |W_{tot}^{-}|$ were respectively the total positive and negative works generated by the entity. $|W_{com}^{-}|$ and $|W_{ext}^{+}|$ where respectively the negative work during the compression phase and the positive work during the extension phase.

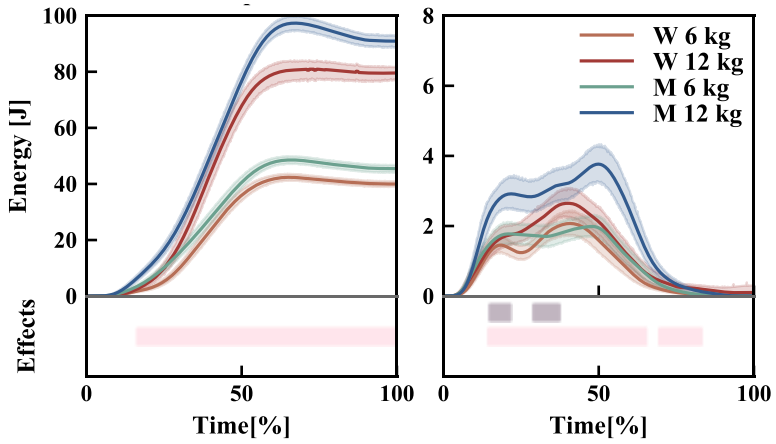


373

374 *Fig. S3.* ***Left****: potential energy of the box with reference at hip level solid line,* ***right****: Kinetic*

375 *energy of the box with the box state at t=0 as reference value: mean value, hue: 95% confidence*

376 *interval, pink bands: load effect, purple bands: sex-load effect.*

377 *Note: The difference in potential energy between men and women was due to the height of the*

378 *shelves that has been normalized to participants height (women: 167.7±7.1 cm, men: 179.3±7.9*

379 *cm).*

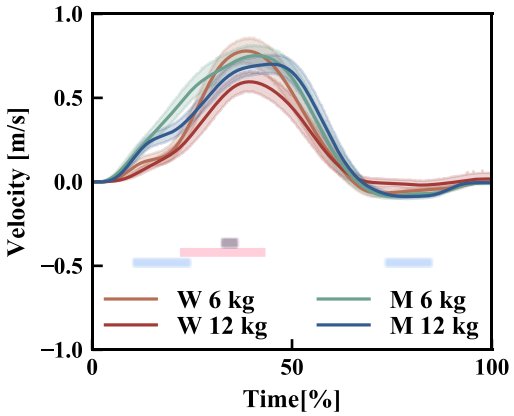


380

381 *Fig. S4. Vertical velocity of the box (6 or 12 kg) for women (W) and men (M): solid line: mean value,*

382 *hue: 95% confidence interval, blue bands: sex effect, pink bands: load effect, purple bands: sex-load*

383 *effect.*

## ACKNOWLEDGMENT

This research was undertaken thanks, in part to funding from the Canada First Research Excellence Fund through the TransMedTech Institute. We acknowledge the support of the Natural Sciences and Engineering Research Council of Canada (NSERC), [RGPIN-2019-04978]. This study was carried out within the framework of the Associated International Laboratory EVASYM.

## CONFLICT OF INTEREST

The authors do not have any conflict of interest that could inappropriately influence this manuscript.

Aagaard, P., 2018. Spinal and supraspinal control of motor function during maximal eccentric muscle contraction: Effects of resistance training. Journal of Sport and Health Science 7, 282–293. https://doi.org/10.1016/j.jshs.2018.06.003

Arias-Martorell, J., 2019. The morphology and evolutionary history of the glenohumeral joint of hominoids: A review. Ecology and Evolution 9, 703–722. https://doi.org/10.1002/ece3.4392

Assila, N., Pizzolato, C., Martinez, R., Lloyd, D.G., Begon, M., 2020. EMG-Assisted Algorithm to Account for Shoulder Muscles Co-Contraction in Overhead Manual Handling. Applied Sciences 10, 3522. https://doi.org/10.3390/app10103522

Balogh, I., Arvidsson, I., Björk, J., Hansson, G.-Å., Ohlsson, K., Skerfving, S., Nordander, C., 2019. Work-related neck and upper limb disorders – quantitative exposure–response relationships adjusted for personal characteristics and psychosocial conditions. BMC Musculoskeletal Disorders 20, 139. https://doi.org/10.1186/s12891-019-2491-6

Biewener, A.A., 2016. Locomotion as an emergent property of muscle contractile dynamics. J Exp Biol 219, 285–294. https://doi.org/10.1242/jeb.123935

Biewener, A.A., 2009. Muscle and Tendon Energy Storage, in: Binder, M.D., Hirokawa, N., Windhorst, U. (Eds.), Encyclopedia of Neuroscience. Springer, Berlin, Heidelberg, pp. 2492–2496. https://doi.org/10.1007/978-3-540-29678-2_3657

Blache, Y., Dumas, R., Lundberg, A., Begon, M., 2016. Main component of soft tissue artifact of the upper-limbs with respect to different functional, daily life and sports movements. J. Biomech. https://doi.org/10.1016/j.jbiomech.2016.10.019

Bouffard, J., Martinez, R., Plamondon, A., Côté, J.N., Begon, M., 2019. Sex differences in glenohumeral muscle activation and coactivation during a box lifting task. Ergonomics 1–12. https://doi.org/10.1080/00140139.2019.1640396

Brent, R.P., 1973. Some Efficient Algorithms for Solving Systems of Nonlinear Equations. SIAM J. Numer. Anal. 10, 327–344. https://doi.org/10.1137/0710031

Burkart, A.C., Debski, R.E., 2002. Anatomy and Function of the Glenohumeral Ligaments in Anterior Shoulder Instability. Clinical Orthopaedics and Related Research® 400, 32.

Dal Maso, F., Marion, P., Begon, M., 2016. Optimal Combinations of Isometric Normalization Tests for the Production of Maximum Voluntary Activation of the Shoulder Muscles. Arch. Phys. Med. Rehabil. 97, 1542-1551.e2. https://doi.org/10.1016/j.apmr.2015.12.024

Davies, G.J., Matheson, J.W., 2001. Shoulder Plyometrics. Sports Medicine and Arthroscopy Review 9, 1–18.

Delp, S.L., Anderson, F.C., Arnold, A.S., Loan, P., Habib, A., John, C.T., Guendelman, E., Thelen, D.G., 2007. OpenSim: Open-Source Software to Create and Analyze Dynamic Simulations of Movement. IEEE Trans. Biomed. Eng. 54, 1940–1950. https://doi.org/10.1109/TBME.2007.901024

Dickinson, M.H., Farley, C.T., Full, R.J., Koehl, M. a. R., Kram, R., Lehman, S., 2000. How Animals Move: An Integrative View. Science 288, 100–106. https://doi.org/10.1126/science.288.5463.100

Fenwick, A.J., Wood, A.M., Tanner, B.C.W., 2017. Effects of cross-bridge compliance on the force-velocity relationship and muscle power output. PLoS One 12. https://doi.org/10.1371/journal.pone.0190335

Gobbi, A., 2017. Bio-orthopaedics: a new approach. Springer Berlin Heidelberg, New York, NY.

Guo, L.-Y., Su, F.-C., Wu, H.-W., An, K.-N., 2003. Mechanical energy and power flow of the upper extremity in manual wheelchair propulsion. Clin Biomech 18, 106–114. https://doi.org/10.1016/S0268-0033(02)00177-8

Hawkes, D.H., Khaiyat, O.A., Howard, A.J., Kemp, G.J., Frostick, S.P., 2019. Patterns of muscle coordination during dynamic glenohumeral joint elevation: An EMG study. PLoS ONE 14, e0211800. https://doi.org/10.1371/journal.pone.0211800

Inman, V.T., Saunders, J.B. dec M., Abbott, L.C., 1996. Observations of the Function of the Shoulder Joint. Clinical Orthopaedics and Related Research® 330, 3.

Jackson, M., Michaud, B., Tétreault, P., Begon, M., 2012. Improvements in measuring shoulder joint kinematics. J. Biomech. 45, 2180–2183. https://doi.org/10.1016/j.jbiomech.2012.05.042

Janssen, I., Heymsfield, S.B., Wang, Z., Ross, R., 2000. Skeletal muscle mass and distribution in 468 men and women aged 18–88 yr. Journal of Applied Physiology 89, 81–88. https://doi.org/10.1152/jappl.2000.89.1.81

Kubo, K., Kanehisa, H., Fukunaga, T., 2003. Gender differences in the viscoelastic properties of tendon structures. Eur J Appl Physiol 88, 520–526. https://doi.org/10.1007/s00421-002-0744-8

Lai, A.K.M., Biewener, A.A., Makeling, J.M., 2019. Muscle-specific indices to characterise the functional behaviour of human lower-limb muscles during locomotion. J. Biomech. 89, 134–38. https://doi.org/10.1016/j.jbiomech.2019.04.027

Lappin, A.K., Monroy, J.A., Pilarski, J.Q., Zepnewski, E.D., Pierotti, D.J., Nishikawa, K.C., 2006. Storage and recovery of elastic potential energy powers ballistic prey capture in toads. Journal of Experimental Biology 209, 2535–2553. https://doi.org/10.1242/jeb.02276

Larson, S.G., 2009. Evolution of the Hominin Shoulder: Early Homo, in: Grine, F.E., Fleagle, J.G., Leakey, R.E. (Eds.), The First Humans – Origin and Early Evolution of the Genus Homo. Springer Netherlands, Dordrecht, pp. 65–75. https://doi.org/10.1007/978-1-4020-9980-9_7

Lee, S.-B., An, K.-N., 2002. Dynamic Glenohumeral Stability Provided by Three Heads of the Deltoid Muscle. Clinical Orthopaedics and Related Research® 400, 40.

Ludewig, P.M., Phadke, V., Braman, J.P., Hassett, D.R., Cieminski, C.J., LaPrade, R.F., 2009. Motion of the Shoulder Complex During Multiplanar Humeral Elevation. J Bone Joint Surg Am 91, 378–389. https://doi.org/10.2106/JBJS.G.01483

Martinez, R., Assila, N., Goubault, E., Begon, M., 2020. Sex differences in upper limb musculoskeletal biomechanics during a lifting task. Applied Ergonomics 86, 103106. https://doi.org/10.1016/j.apergo.2020.103106

Martinez, R., Bouffard, J., Michaud, B., Plamondon, A., Côté, J.N., Begon, M., 2019. Sex differences in upper limb 3D joint contributions during a lifting task. Ergonomics 62, 682–693. https://doi.org/10.1080/00140139.2019.1571245

Pataky, T.C., Vanrenterghem, J., Robinson, M.A., 2015. Zero- vs. one-dimensional, parametric vs. non-parametric, and confidence interval vs. hypothesis testing procedures in one-dimensional biomechanical trajectory analysis. Journal of Biomechanics 48, 1277–1285. https://doi.org/10.1016/j.jbiomech.2015.02.051

Pizzolato, C., Lloyd, D.G., Sartori, M., Ceseracciu, E., Besier, T.F., Fregly, B.J., Reggiani, M., 2015. CEINMS: A toolbox to investigate the influence of different neural control solutions on the prediction of muscle excitation and joint moments during dynamic motor tasks. J. Biomech. 48, 3929–3936. https://doi.org/10.1016/j.jbiomech.2015.09.021

Qiao, M., Jindrich, D.L., 2016. Leg joint function during walking acceleration and deceleration. Journal of Biomechanics 49, 66–72. https://doi.org/10.1016/j.jbiomech.2015.11.022

Raiteri, B.J., Cresswell, A.G., Lichtwark, G.A., 2018. Muscle-tendon length and force affect human tibialis anterior central aponeurosis stiffness in vivo. PNAS 115, E3097–E3105. https://doi.org/10.1073/pnas.1712697115

Richardson, A.G., Slotine, J.-J.E., Bizzi, E., Tresch, M.C., 2005. Intrinsic Musculoskeletal Properties Stabilize Wiping Movements in the Spinalized Frog. J. Neurosci. 25, 3181–3191. https://doi.org/10.1523/JNEUROSCI.4945-04.2005

Roach, N.T., Venkadesan, M., Rainbow, M.J., Lieberman, D.E., 2013. Elastic energy storage in the shoulder and the evolution of high-speed throwing in Homo. Nature 498, 483–486. https://doi.org/10.1038/nature12267

Sangwan, S., Green, R.A., Taylor, N.F., 2015. Stabilizing characteristics of rotator cuff muscles: a systematic review. Disability and Rehabilitation 37, 1033–1043. https://doi.org/10.3109/09638288.2014.949357

Sartori, M., Farina, D., Lloyd, D.G., 2014. Hybrid neuromusculoskeletal modeling to best track joint moments using a balance between muscle excitations derived from electromyograms and optimization. J. Biomech. 47, 3613–3621. https://doi.org/10.1016/j.jbiomech.2014.10.009

Siegel, K.L., Kepple, T.M., Stanhope, S.J., 2004. Joint moment control of mechanical energy flow during normal gait. Gait & Posture 19, 69–75. https://doi.org/10.1016/S0966-6362(03)00010-9

Stokdijk, M., Eilers, P.H.C., Nagels, J., Rozing, P.M., 2003. External rotation in the glenohumeral joint during elevation of the arm. Clinical Biomechanics 18, 296–302. https://doi.org/10.1016/S0268-0033(03)00017-2

Tillin, N.A., Pain, M.T.G., Folland, J.P., 2018. Contraction speed and type influences rapid utilisation of available muscle force: neural and contractile mechanisms. J Exp Biol 221, jeb193367. https://doi.org/10.1242/jeb.193367

Veeger, H.E.J., van der Helm, F.C.T., 2007. Shoulder function: The perfect compromise between mobility and stability. J. Biomech 40, 2119–2129. https://doi.org/10.1016/j.jbiomech.2006.10.016

Wilk, K.E., Arrigo, C.A., Andrews, J.R., 1997. Current Concepts: The Stabilizing Structures of the Glenohumeral Joint. J Orthop Sports Phys Ther 25, 364–379. https://doi.org/10.2519/jospt.1997.25.6.364

Wilkie, D.R., 1975. Muscle as a thermodynamic machine. Ciba Found. Symp. 327–339.

Wu, G., van der Helm, F.C.T., Veeger, H.E.J.D., Makhsous, M., Van Roy, P., Anglin, C., Nagels, J., Karduna, A.R., McQuade, K., Wang, X., Werner, F.W., Buchholz, B., International Society of Biomechanics, 2005. ISB recommendation on definitions of

joint coordinate systems of various joints for the reporting of human joint motion--Part II: shoulder, elbow, wrist and hand. J Biomech 38, 981–992.

Wu, W., Lee, P.V.S., Bryant, A.L., Galea, M., Ackland, D.C., 2016. Subject-specific musculoskeletal modeling in the evaluation of shoulder muscle and joint function. J. Biomech. 49, 3626–3634. https://doi.org/10.1016/j.jbiomech.2016.09.025

Yanagawa, T., Goodwin, C.J., Shelburne, K.B., Giphart, J.E., Torry, M.R., Pandy, M.G., 2008. Contributions of the Individual Muscles of the Shoulder to Glenohumeral Joint Stability During Abduction. J Biomech Eng 130. https://doi.org/10.1115/1.2903422

Yang, C., Leitkam, S., Côté, J.N., 2019. Effects of different fatigue locations on upper body kinematics and inter-joint coordination in a repetitive pointing task. PLOS ONE 14, e0227247. https://doi.org/10.1371/journal.pone.0227247